Longitudinal profile of channels cut by springs

O. Devauchelle, A. P. Petroff, A. E. Lobkovsky, D. H. Rothman

Longitudinal profile of channels cut by springs

By O. DEVAUCHELLE, A. PETROFF, A. E. LOBKOVSKY, and D. H. ROTHMAN

Department of Earth, Atmospheric and Planetary Sciences, Massachusetts Institute of Technology, 77 Massachusetts Avenue, Cambridge MA 02139-4307, USA

(Received 17 September 2010)

We propose a simple theory for the longitudinal profile of channels incised by groundwater flow. The aquifer surrounding the stream is represented in two dimensions through Darcy's law and the Dupuit approximation. The model is based on the assumption that, everywhere in the stream, the shear stress exerted on the sediment by the flow is close to the minimal intensity required to displace a sand grain. Due to the coupling of the stream discharge with the water table elevation in the neighbourhood of the channel head, the stream elevation decreases as the distance from the stream's tip with an exponent of 2/3. Field measurements of steephead ravines in the Florida panhandle conform well to this prediction.

1. Introduction

In his study of the badlands of the Henry Mountains, Gilbert (1877) noted that "*if we draw the profile of the river on paper, we produce a curve concave upward and with the greatest curvature at the upper end*" (p. 116). In fact, the concavity of the longitudinal profile of rivers is a general feature of landscapes despite the wide range of the processes involved in shaping rivers (Sinha & Parker 1996). The local slope of a river is set primarily by its discharge, width and sediment size distribution, and by the rate at which it transports sediment. Its profile thus results from its interaction with the surrounding topography which supplies water and sediment to the stream (Snow & Slingerland 1987). As a landscape responds to climatic and tectonic perturbations, the profiles of streams can bear the geomorphological signature of ancient forcing (Whipple 2001). More generally, the profile of a river reflects the way it incises a landscape. A quantitative theory of longitudinal profiles could improve our understanding of how a drainage network grows and organizes itself.

Various mechanisms have been proposed to explain the concavity of river profiles, ranging from the accumulation of water and sediment discharges from tributaries (Snow & Slingerland 1987; Rice & Church 2001) to the equilibrium between basin subsidence and sediment deposition by the river (Paola *et al.* 1992). In addition to these mechanisms, most models also involve the downstream fining of the bed sediment, the role of which is broadly acknowledged (Sklar & Dietrich 2008). To better understand which, if any of these mechanisms are quantitatively important, we focus on a simpler geological system: ravines formed by groundwater sapping in uniform sand (Dunne 1980; Howard 1988; Schumm *et al.* 1995; Lamb *et al.* 2008). Sapping occurs when groundwater seeps from porous ground with enough strength to detach sediment grains, and to transport them further downstream (Howard & McLane III 1988; Fox *et al.* 2007). This process causes

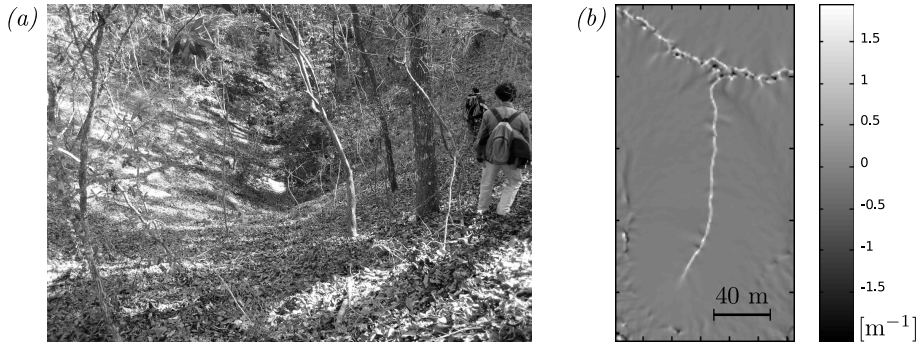

FIGURE 1. Steepheads in the Apalachicola Bluffs and Ravines Preserve. *(a)* Picture of the amphitheatre head. The spring is located approximately in the middle of the picture. *(b)* Curvature of the elevation contours. A strong curvature (light grey) reveals the presence of a stream. Mapping data were collected by the National Center for Airborne Laser Mapping (Abrams *et al.* 2009).

the soil above the seepage face to collapse, thus forming a receding erosion front as the valley head advances, often used to identify sapping as the incision mechanism (Higgins 1982; Laity & Malin 1985; Kochel & Piper 1986), but not without controversy (Lamb *et al.* 2006, 2008; Petroff *et al.* 2009).

The advance of the valley head through the porous ground creates a ravine, at the bottom of which flows a stream fed by the surrounding aquifer. Here we present a simple analytical model of the interaction between sediment transport in the stream and the aquifer. We use the marginal stability hypothesis for sediment transport and the assumption of fully turbulent flow to derive a relationship between the flux of water carried by the stream and its longitudinal slope. This relationship serves as the boundary condition for the water table elevation which allows us to compute the water flux and the stream profile near the head. This theory concerns first-order streams, that is, the stream segments between a tip and the first confluence. Finally, the model is tested against thirteen streams from a single field site, described in section 2. The shape of the mean longitudinal profile of the streams is well predicted by our theory.

2. The Apalachicola ravines

The so-called steephead ravines of the Florida panhandle are 20 to 40 m deep and about 100 m wide, cut in sand by groundwater sapping (Schumm *et al.* 1995; Abrams *et al.* 2009). Because of their unambiguous origin and the relative simplicity of their geological substrate, we use them as an inspiration for the present theory. Beautiful specimens of steepheads are found in the Apalachicola Bluffs and Ravines Preserve, north of Bristol, Florida. At their head, a spring is surrounded by an amphitheatre-shaped sand bluff nearly at the angle of repose. Because of this typical structure, the tip of a first-order stream is well-defined, a property crucial to our analysis (figure 1).

The Florida steepheads form in a layer of reasonably homogeneous quartz sand of about 0.45 mm in diameter. Schmidt (1985) provides a stratigraphic column showing that a surficial 15 m-thick layer of sand is supported by less permeable clay layers, the uppermost of which lies about 30 m above sea level. As a first approximation, we extrapolate this value to the entire network and assume it is the base of the aquifer.

The hydraulic conductivity K of the sand is high enough for the soil to absorb the rain water before runoff can develop (there are almost no visible erosion rills on the

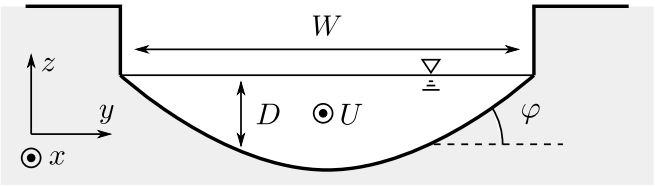

FIGURE 2. Schematics of a stream section. The notations are defined in section 3.1.

ground). In addition, the characteristic time scale of the aquifer is long enough to damp out most of the seasonal variations in the precipitation rate (Petroff *et al.* 2009), and the discharge of the stream is rather constant except during extreme rain events. The theory developed here is based on the assumption that the average discharges have a stronger impact on the stream morphology than extreme events (Wolman & Miller 1960), and consequently we consider hereafter a uniform precipitation rate of about $P \approx 4.6 \times 10^{-8}$ m s^{-1}. Conversely, since clay is about ten thousand times less permeable than the sand (Bear 1988), it can be considered an impervious aquitard as a first approximation. As the slope of the stream is moderate (typically 10^{-2}), we can use Dupuit's approximation to relate the groundwater flux to the elevation of the water table (Dupuit 1863; Bear 1988):

$$\mathbf{q}_w = -Kh\boldsymbol{\nabla}h, \tag{2.1}$$

where $\mathbf{q}_w$, K and h denote the groundwater flux (in the horizontal plane), the sand conductivity, and the aquifer thickness respectively. The water mass balance then dictates that the squared water table elevation satisfies Poisson's equation (Bear 1988):

$$\nabla^2 h^2 = -\frac{2P}{K}. \tag{2.2}$$

Petroff *et al.* (2009) show that the discharge predicted by the above equation compares well to 85 flow measurements at different locations along the Florida network. The discharge was deduced from the local geometry of the channel and the surface water velocity, which was measured using passive tracers. The same data are used in section 3.2 to support intermediate steps of the present theory.

3. Coupling groundwater flow to sediment transport

We first derive a relation between the slope S and the discharge Q_w of a stream, through the simplest possible model for a turbulent flow int the streams. Next, in section 3.2, we show that the coupling of this relation to Duipuit's representation of the aquifer surrounding the stream imposes the shape of the stream profile.

3.1. *Streams*

Lane (1955) and Henderson (1961) suggested that the stable width of a channel is selected mainly by the mechanical equilibrium of sediment grains. In other words, the sum of the constraints applied to the bed by the flow and by gravity amounts exactly to the level required to move a grain, an idea which can be extended to different sediment transport modes (Dade 2000). Strictly speaking, this hypothesis implies that no sediment is transported by the stream. However, this approximation can be interpreted in a more flexible way by assuming that the Shields parameter, defined below, remains close to the threshold value for transport, thus allowing for some bedload transport (Parker 1978; Savenije 2003), without departing considerably from the true equilibrium shape.

Following this interpretation, we can determine the shape of an idealized channel exactly at equilibrium, and expect the dimensions of actual channels not to depart strongly from this theoretical cross-section.

Let us define the depth D of a stream at the average disacharge (figure 2). For a shallow channel, the shear stress exerted by the flow on the bed can be approximated by $\rho_w g S D$, where ρ_w and g are the water density and the acceleration of gravity respectively. As established by Henderson (1961), the equilibrium hypothesis then reads

$$\theta_t = \frac{\sqrt{(RSD/d_s)^2 + \sin^2\varphi}}{\cos\varphi}, \tag{3.1}$$

where θ_t is the threshold Shields parameter, $R = \rho_w/(\rho_s - \rho_w) \approx 0.61$ compares the density of the sediment ρ_s to the density of water, $d_s \approx 0.45$ mm is the average grain size, and φ is the lateral bed slope. The right-hand side of the above equation corresponds to the ratio of the forces tangential to the bed to the normal forces. It can be interpreted as a generalization of the classical Shields parameter (Devauchelle *et al.* 2009). If the square of the threshold Shields parameter θ_t^2 is small, then equation (3.1) leads to a shallow channel :

$$D = \frac{\theta_t d_s}{SR} \cos\left(\frac{SRy}{d_s}\right), \tag{3.2}$$

where y denotes the transverse coordinate. Consequently, the channel aspect ratio is $W/\langle D\rangle = \pi^2/(2\theta_t)$, where W and $\langle D\rangle$ are the width and the mean depth of the channel, respectively.

The field data presented in figure 3a indicate a strong correlation between the width and the depth of a stream, with a Spearman rank correlation coefficient of 0.92. Each point on the plot represents an average over a few measurements at a given location. Fitting a power-law $W \propto \langle D\rangle^p$, yields $p = 0.97 \pm 0.04$. These measurements thus support the mechanical equilibrium theory, which predicts that width and depth are linearly related. The mean aspect ratio of the streams is found to be 16.7 ± 0.7, which corresponds to a threshold Shields parameter of about $\theta_t \approx 0.29$. Lobkovsky *et al.* (2008) showed experimentally that a flume stops eroding its bed when the Shields parameter reaches a value of about 0.30.

A few meters from the spring, the Reynolds number of the streams is of the order of 10^4, and increases downstream. The Darcy–Weisbach relation applied to a turbulent, stationary and spatially invariant flow states that (Chanson 2004):

$$\sqrt{gDS} = C_f U, \tag{3.3}$$

where U is the depth-averaged velocity of water, and C_f is the friction factor. The value of the latter is known to depend on the ratio of the bed roughness z_0 to the flow depth D. A common approximation is, for instance (Katul *et al.* 2002)

$$C_f \approx 0.18 \left(\frac{z_0}{D}\right)^{1/7}. \tag{3.4}$$

The roughness length of a sand bed is set by the grain size (Katul *et al.* 2002). In the streams of the Appalachicola Reserve, we expect the bed roughness of about $z_0 \sim 0.45$ mm. According to equation (3.4), we expect the friction factor C_f to vary between 0.10 and 0.18 in the streams corresponding to the data set presented on figure 3, with an average of 0.14. For the sake of simplicity, the friction factor C_f will be treated as a constant hereafter, but a more elaborate model could include its variation.

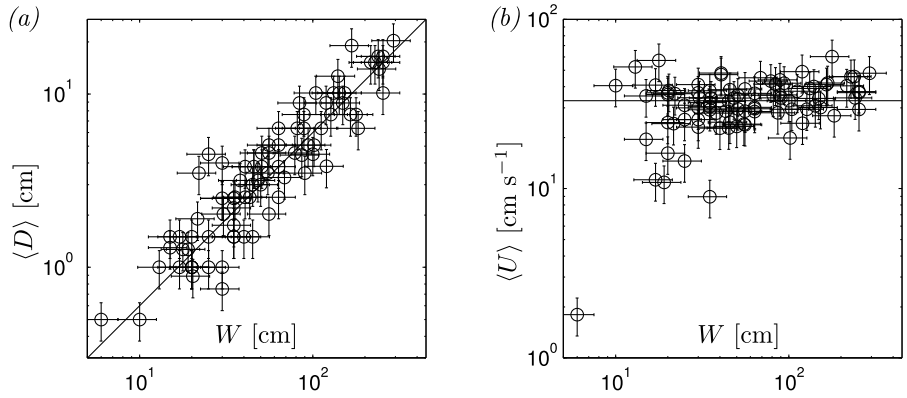

FIGURE 3. *(a)* Stream depth versus stream width for 85 streams of the Apalachicola Bluffs and Ravines Preserve. The solid line represents the best proportionality relation between the two quantities, namely $W = 16.7\langle D \rangle$. *(b)* Velocity of a stream versus its width. The average velocity, represented by a solid line, is 33.0 cm s^{-1}. The bars indicate the estimated measurement error. The lowest data point corresponds to a laminar stream.

Combining equations (3.2) and (3.3), we find that the mean velocity of a stream is

$$\langle U \rangle = \frac{2\sqrt{2}\,\Gamma^2(3/4)}{\pi^{3/2} C_f} \sqrt{\frac{g\theta_t d_s}{R}} \approx \frac{0.76}{C_f} \sqrt{\frac{g\theta_t d_s}{R}}, \tag{3.5}$$

where Γ denotes the Euler gamma function. At first order, the water velocity depends only on the grain size, and thus should remain constant throughout the network, if the friction factor is constant. The velocity measurements presented in figure 3b have a mean of 33 ± 1 cm s^{-1}, corresponding to a friction factor $C_f \approx 0.11$, which lies within the expected range. Alternatively, one could attempt to fit a power-law to figure 3b, but the correlation between W and $\langle U \rangle$ is too small (the rank correlation coefficient is 0.29) to justify a non-constant velocity.

Finally, from equations (3.2) and (3.3), we can relate the water discharge Q_w to the stream slope S, after averaging over the channel width:

$$\begin{aligned} Q_w S^2 &= \frac{2\sqrt{2}\,\mathcal{K}(1/2)}{3C_f} \sqrt{\theta_t^3 g \left(\frac{d_s}{R}\right)^5} \\ &\approx \frac{1.75}{C_f} \sqrt{\theta_t^3 g \left(\frac{d_s}{R}\right)^5} \\ &\equiv Q_0, \end{aligned} \tag{3.6}$$

where $\mathcal{K}$ is the complete elliptic integral of the first kind. In the Florida network, $Q_0 \approx 1.2 \times 10^{-7}$ m^{3}s^{-1}, which is consistent with the typical value of the slope $S \sim 10^{-2}$ and of the discharge $Q_w \sim 10^{-3}$ m^{3}s^{-1} observed in the field. The above slope–discharge relation is reminiscent of the empirical relations of Leopold & Wolman (1957) for alluvial rivers at equilibrium. Inasmuch as the type of sediment does not vary along the stream, Q_0 remains constant. Since most rivers accumulate water downstream, equation (3.6) imposes a concave longitudinal profile. As pointed out by Savenije (2003) and Henderson (1961), the above model also relates the river width W to its discharge Q_w through

$$W = \pi \left(\frac{R}{\theta_t^3 d_s}\right)^{1/4} \sqrt{\frac{3C_f Q_w}{2\sqrt{2}\,\mathcal{K}(1/2)\, g}}. \tag{3.7}$$

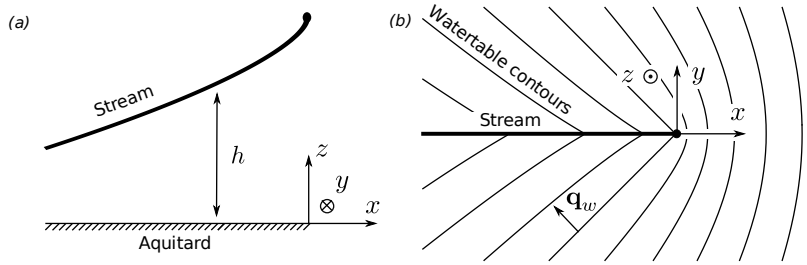

FIGURE 4. Schematics of a channel tip, *(a)* from side and *(b)* from above.

The proportionality of the width to the square root of the discharge, sometimes referred to as to Lacey's formula, has been supported both in the field and in laboratory experiments by Fourrière (2009).

At scales much larger than the river width, relation (3.6) is a boundary condition for the Poisson equation controlling the water table elevation around the streams, since it imposes a relation between the water flux seeping into the river, and the longitudinal slope of the boundary itself. Indeed, if s denotes the arclength along a stream starting from the tip, then

$$Q_w = K \int_0^s h \left(\frac{\partial h_r}{\partial n} + \frac{\partial h_l}{\partial n} \right) ds' \quad \text{and} \quad S = \frac{\partial h}{\partial s}, \tag{3.8}$$

where $\partial/\partial n$ denotes a derivative with respect to the transversal direction, and the subscripts r and l represent the right-hand side and the left-hand side of a stream, respectively. We thus expect the water table to evolve in conjunction with the river, through erosion, to match this boundary condition. The following section is devoted to determining the behaviour of the equilibrium solution in the neighbourhood of a river tip.

3.2. *Groundwater*

Through the Poisson equation (2.2) and the boundary condition (3.6), the longitudinal profile of a stream depends on the position of all other streams within the network. Nonetheless, some general conclusions can be drawn from the knowledge of the water table near the tip. The coordinates are chosen such that the stream corresponds to the half axis $(-\infty, 0]$ (figure 4). The squared water table elevation can be divided into a homogeneous and an inhomogeneous part by means of the following definition:

$$h^2 = \phi - \frac{P y^2}{K}. \tag{3.9}$$

The homogeneous solution ϕ must satisfy both the boundary condition (3.6), to which the inhomogeneous solution $-Py^2/K$ does not contribute, and the Laplace equation $\nabla^2 \phi = 0$. For an absorbing boundary condition, the Laplace equation produces a square-root singularity around needles (Churchill & Brown 1984). Based upon this classical example, and since ϕ is an analytic function of $\zeta = x + iy$, we propose the following expansion near the tip:

$$\phi \sim h_0^2 \, \mathrm{Re} \left(1 + \left(\frac{\zeta}{L} \right)^\alpha \right) \tag{3.10}$$

where h_0 is the elevation of the tip, L is a length to be determined, and α is a dimensionless parameter. If s is the distance from the tip, then along the river $\zeta = s e^{i\pi}$. Therefore,

at leading order, the profile h, the slope S and the discharge Q_w of the stream read

$$h \sim h_0 \left(1 + \frac{\cos(\alpha\pi)}{2} \left(\frac{s}{L}\right)^{\alpha}\right), \tag{3.11}$$

$$S \sim \frac{\alpha h_0 \cos(\alpha\pi) s^{\alpha-1}}{2L^{\alpha}}, \quad Q_w \sim K h_0^2 \sin(\alpha\pi) \left(\frac{s}{L}\right)^{\alpha}. \tag{3.12}$$

Finally, the boundary condition (3.6) imposes

$$\alpha = \frac{2}{3}, \quad L = \frac{h_0^2}{2\sqrt{2\sqrt{3^3}}} \sqrt{\frac{K}{Q_0}}. \tag{3.13}$$

The river profile thus behaves as a power-law near the tip, with an exponent of 2/3:

$$h = h_0 - \frac{\sqrt{3}}{2} \left(\frac{Q_0}{K h_0}\right)^{1/3} s^{2/3}. \tag{3.14}$$

The river profile and the watertable contours of figure 4 correspond to the real part of $\zeta^{2/3}$. It is noticeable that the non-homogeneous term of the solution, defined in equation (3.9), is negligible with respect to the expansion (3.14). Both precipitation and the distant boundary conditions are encoded into the coefficient of the leading order term only through Q_0.

4. Comparison with field data

Among the approximately 100 valley heads of the Bristol ravine network, we have selected the 13 streams presented in figure 5a by reason of their sufficient length and the absence of tip-splitting or strong planform curvature. The accuracy of our topographic map, about 1 m horizontally and 5 cm vertically (Abrams *et al.* 2009), allows us to follow the flow path and elevation of individual channels. The position of the tips was manually determined from the contour curvature map (figure 1). The corresponding profile $h(s)$, including the spring elevation h_0, is then calculated by means of a steepest descent algorithm. The main uncertainty when evaluating h is the depth of the aquitard (see section 2).

Each individual stream profile, when plotted in the log-log space (figure 5b), presents an average slope smaller than one, indicative of a positive concavity consistent with equation (3.14). More precisely, if a power-law is fit to each profile, the 13 exponents are distributed between 0.45 and 0.83, with a mean of 0.660 and a standard deviation of 0.12. Thus the profiles are distributed around the 2/3 power-law of equation (3.14) with important dispersion. This scatter is not surprising as we consider individual streams. In particular, local variations in the average ground conductivity K, or in the elevation of the aquitard (which influences the data through the evaluation of h_0) can explain this dispersion. We did not find any visible pattern in the spatial distribution of prefactors throughout the network.

We then calculate the geometric mean of the 13 individual profiles (dark grey circles on figure 5b). A least squares fit of the resulting mean profile leads to an exponent of 0.693 ± 0.004, slightly above the theoretical value of 2/3. If we consider the influence of depth on the friction coefficient through equation (3.4), then the theoretical exponent α would be $15/22 \approx 0.682$ instead of 2/3. As expected the average profile compares much more favorably with theory than does any individual channel, suggesting that local geological variations cause the dispersion of the data.

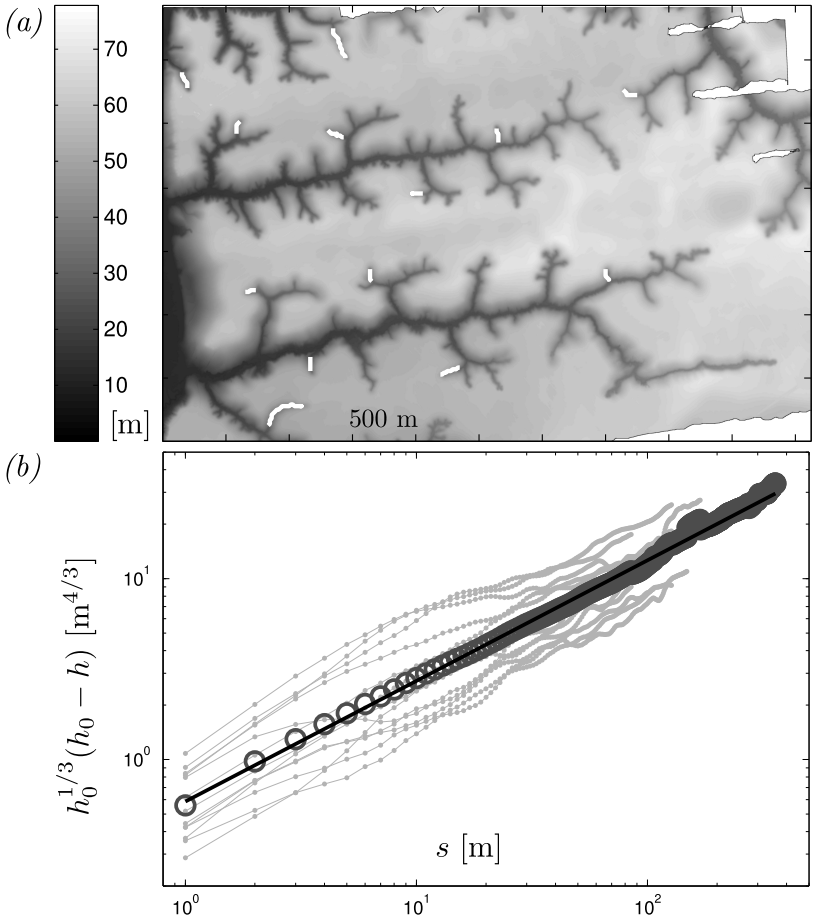

FIGURE 5. *(a)* Topographic map of the Bristol channel network. The grey scale corresponds to elevation. The white lines indicate the position of the streams for which the profiles are compared to theory. *(b)* Longitudinal profiles of the rivers presented in figure 5a (grey lines). The dark grey circles are the geometrical mean of the elevation over the 13 streams. The black line represents equation (3.14) with $Q_0/K = 0.347$ m^2.

Finally, if the prefactor of the theoretical profile (3.14) is adjusted to the data (black line on figure 5), we find $Q_0/K = 0.347 \pm 0.003$ m^2, which corresponds to conductivity of about 3.6×10^{-7} m s^{-1}, a value corresponding to very fine sand. If clean and not compacted, one would expect a conductivity of about 10^{-4} m s^{-1}(Bear 1988) for the sand of the Florida network. The presence of organic materials and clay lenses in the stratigraphy might explain this result.

5. Discussion and conclusion

We have developed a simple analytical model representing the interaction between an alluvial stream formed by seepage and the surrounding water table. The coupling occurs through a slope–discharge relation derived from a simple stream model. This theory predicts that the longitudinal stream profile near the spring should decrease like the distance from the tip, with an exponent of 2/3. This power-law relation has been successfully tested against data from a well-understood field site.

Besides the asymptotic expansion presented in section 3.2, this theory can be applied to more complex systems, such as a complete network of streams cut by seepage. If the position of the streams is specified, then their profiles can be computed by solving the Poisson equation with a non-linear boundary condition. By specifying a relation between the intensity of the water discharge and the advance rate of a channel head, one might describe the formation of a seepage channel network in a way resembling dendrite growth models (Derrida & Hakim 1992). Nonetheless, this model differs from classical needle growth in Laplacian fields in two ways. First, the non-vanishing divergence of the water flux due to precipitation allows the stream heads to collect water (and thus to grow) even when they undergo the screening effect of other needles. Second, the requirement that the stream be at equilibrium with respect to sediment transport can restrict its growth even when it collects a large amount of water from the aquifer. Based upon these considerations, we expect that the statistical properties of a seepage network would differ significantly from classical dendrites.

Finally, even though the present contribution focuses on a very specific geological system, it is nevertheless related to river networks formed by runoff, a more common situation (Perron *et al.* 2009; Fowler *et al.* 2007). Indeed, if the topography of an eroding landscape undergoes diffusion while tectonic uplift generates a uniform injection of sediment, the stationary state of the landscape can be represented by the Poisson equation. Assuming additionally that runoff follows the main slope of the topography, one recovers a theory that is mathematically equivalent to the seepage model of this paper.

We would like to thank The Nature Conservancy for access to the Apalachicola Bluffs and Ravines Preserve. It is also our pleasure to thank D. M. Abrams, M. Berhanu, D. J. Jerolmack, A. Kudrolli, D. Lague, E. Lajeunesse and B. McElroy for fruitful discussions. This work was supported by Department of Energy grant FG02-99ER15004. O. D. was supported by the French Academy of Sciences.

REFERENCES

Abrams, D. M., Lobkovsky, A. E., Petroff, A. P., Straub, K. M., McElroy, B., Mohrig, D. C., Kudrolli, A. & Rothman, D. H. 2009 Growth laws for channel networks incised by groundwater flow. *Nature Geoscience* **2**, 193–196.

Bear, J. 1988 *Dynamics of fluids in porous media*. Dover Publications.

Chanson, H. 2004 *The hydraulics of open channel flow: an introduction*, 2nd edn. Elsevier Butterworth-Heinemann.

Churchill, R. V. & Brown, J. W. 1984 *Complex variables and applications*. McGraw-Hill Book Company.

Dade, W. B. 2000 Grain size, sediment transport and alluvial channel pattern. *Geomorphology* **35** (1-2), 119–126.

Derrida, B. & Hakim, V. 1992 Needle models of Laplacian growth. *Physical Review A* **45** (12), 8759–8765.

Devauchelle, O., Malverti, L., Lajeunesse, É., Lagrée, P.Y., Josserand, C. & Thu-Lam, K.D.N. 2009 Stability of bedforms in laminar flows with free surface: from bars to ripples. *Journal of Fluid Mechanics* **642**, 329–348.

Dunne, T. 1980 Formation and controls of channel networks. *Progress in Physical Geography* **4** (2), 211.

Dupuit, J. 1863 *Études théoriques et pratiques sur le mouvement des eaux dans les canaux découverts et à travers les terrains perméables*, 2nd edn. Paris: Dunod.

Fourrière, A. 2009 Morphodynamique des rivières: Sélection de la largeur, rides et dunes. Ph.D. thesis, Université Paris Diderot.

Fowler, A. C., Kopteva, N. & Oakley, C. 2007 The formation of river channels. *SIAM Journal on Applied Mathematics* **67** (4), 1016–1040.

Fox, G. A., Chu-Agor, M. L. M. & Wilson, G. V. 2007 Erosion of Noncohesive Sediment by Ground Water Seepage: Lysimeter Experiments and Stability Modeling. *Soil Science Society of America Journal* **71** (6), 1822–1830.

Gilbert, G. K. 1877 *Report on the Geology of the Henry Mountains*. Washington: Government Printing Office.

Henderson, F. M. 1961 Stability of alluvial channels. *J. Hydraulics Div., ASCE* **87**, 109–138.

Higgins, C. G. 1982 Drainage systems developed by sapping on Earth and Mars. *Geology* **10** (3), 147–152.

Howard, A.D. 1988 Groundwater sapping experiments and modeling. *Sapping Features of the Colorado Plateau: A Comparative Planetary Geology Field Guide* pp. 71–83.

Howard, A. D. & McLane III, C. F. 1988 Erosion of cohesionless sediment by groundwater seepage. *Water resources research* **24** (10).

Katul, G., Wiberg, P., Albertson, J. & Hornberger, G. 2002 A mixing layer theory for flow resistance in shallow streams. *Water Resources Research* **38** (11), 1250.

Kochel, R. C. & Piper, J. F. 1986 Morphology of large valleys on Hawaii: Evidence for groundwater sapping and comparisons with Martian valleys. *Journal of Geophysical Research* **91** (B13), E175–E192.

Laity, J. E. & Malin, M. C. 1985 Sapping processes and the development of theater-headed valley networks on the Colorado Plateau. *Geological Society of America Bulletin* **96** (2), 203–217.

Lamb, M. P., Dietrich, W. E., Aciego, S. M., DePaolo, D. J. & Manga, M. 2008 Formation of Box Canyon, Idaho, by megaflood: Implications for seepage erosion on Earth and Mars. *Science* **320** (5879), 1067–1070.

Lamb, M. P., Howard, A. D., Johnson, J., Whipple, K. X., Dietrich, W. E. & Perron, J. T. 2006 Can springs cut canyons into rock? *J. Geophys. Res* **111**, E07002.

Lane, E. W. 1955 Design of stable channels. *Transactions of the American Society of Civil Engineers* **120**, 1234–1260.

Leopold, L. B. & Wolman, M. G. 1957 River channel patterns: braided, meandering, and straight. *Geological Survey Professional Paper* **282** (B), 39–85.

Lobkovsky, A. E., Orpe, A. V., Molloy, R., Kudrolli, A. & Rothman, D. H. 2008 Erosion of a granular bed driven by laminar fluid flow. *Journal of Fluid Mechanics* **605**, 47–58.

Paola, C., Heller, P. L. & Angevine, C. L. 1992 The large-scale dynamics of grain-size variation in alluvial basins, 1: Theory. *Basin Research* **4**, 73–73.

Parker, G. 1978 Self-formed straight rivers with equilibrium banks and mobile bed. Part 2. The gravel river. *J. Fluid Mech* **89** (1), 127–146.

Perron, J. T., Kirchner, J. W. & Dietrich, W. E. 2009 Formation of evenly spaced ridges and valleys. *Nature* **460** (7254), 502–505.

Petroff, A. P., Devauchelle, O., Abrams, D., Lobkovsky, A., Kudrolli, A. & Rothman, D. H. 2009 Physical origin of amphitheater shaped valley heads. *in progress* .

Rice, S. P. & Church, M. 2001 Longitudinal profiles in simple alluvial systems. *Water resources research* **37** (2), 417–426.

Savenije, H. H. G. 2003 The width of a bankfull channel; Lacey's formula explained. *Journal of Hydrology* **276** (1-4), 176–183.

Schmidt, W. 1985 Alum bluff, liberty county, florida. Open File Report 9. Florida Geological Survey.

Schumm, S. A., Boyd, K. F., Wolff, C. G. & Spitz, W. J. 1995 A ground-water sapping landscape in the Florida Panhandle. *Geomorphology* **12** (4), 281–297.

Sinha, S. K. & Parker, G. 1996 Causes of concavity in longitudinal profiles of rivers. *Water Resources Research* **32** (5), 1417–1428.

Sklar, L. S. & Dietrich, W. E. 2008 Implications of the saltation-abrasion bedrock incision model for steady-state river longitudinal profile relief and concavity. *Earth Surface Processes and Landforms* **33** (7), 1129–1151.

Snow, R. S. & Slingerland, R. L. 1987 Mathematical modeling of graded river profiles. *The Journal of Geology* **95** (1), 15–33.

Whipple, K. X. 2001 Fluvial landscape response time: how plausible is steady-state denudation? *American Journal of Science* **301** (4-5), 313–325.

Wolman, M. G. & Miller, J. P. 1960 Magnitude and frequency of forces in geomorphic processes. *The Journal of Geology* **68** (1), 54–74.